

## Apatite-Gelatine-Nanocomposite-Superstructures: New Insights into a Biomimetic System of High Complexity

Horst Borrmann, Jürgen Brickmann<sup>1</sup>, Jana Buder, Wilder Carrillo-Cabrera, Patrick Duchstein, Olga Frank-Kamenetskaya<sup>2</sup>, Oliver Hochrein, Ya-Xi Huang, Agnieszka Kawaska, Simon Kokolakis<sup>1</sup>, Theresa Kollmann, Hannes Lichte<sup>3</sup>, Ygit Öztan, Raffaella Paparcone<sup>1</sup>, Tilo Poth<sup>4</sup>, Yurii Prots, Elena Rosseeva, Ulrich Schwarz, Paul Simon, Harald Tlatlik, Dirk Zahn, and Rüdiger Kniep

### Introduction

Biomimetic apatite-gelatine-nanocomposites are of great interest from the point of view of basic research as well as for different areas of medical applications. This interest is specifically fueled by their close chemical and structural relationships to functional materials in the human body (such as bone and teeth). We focused our investigations on fluorapatite-gelatine-nanocomposites. Structures and morphogenetic principles as well as aspects of dental repair applications of such nanocomposites are summarized in a recent review article [1].

With respect to their morphogenetic principles on the  $\mu\text{m}$ -scale the fluorapatite-gelatine-nanocomposites (containing  $\sim 2.3$  wt.-% gelatine) are characterized by a fractal growth mechanism: It starts off from a (perfect) elongated, hexagonal-prismatic seed, proceeds via growing dumbbell states and finally results in a slightly notched sphere. As already assumed [1], the hexagonal-prismatic nanocomposite seed should bear an intrinsic code for its fractal shape development leading to an outgrowth-scenario for the following generations. It was also assumed, that this scenario has its origin in an intrinsic electric dipole field of the composite seed. The existence of a characteristic electric potential around the composite seeds was proven by electron holography. Moreover, this potential was simulated on the basis of the nanocomposite superstructure. Our simulations revealed a qualitatively good agreement with the experimental data [2].

Interactions of the ionic components of fluorapatite with the protein macromolecules in an aqueous environment were investigated in detail at the atomic level [3,4]. It was shown that pre-impregnation of gelatine by calcium ions results in a fixation of calcium inside the triple-helices

thereby increasing their rigidity [5]. Furthermore, the collagen triple-helices induce an orientation control of  $\text{Ca}_3\text{F}$ -motifs of the apatite crystal structure. Here, the  $c$ -axis direction of the apatite motifs is preferably arranged parallel to the long axis of the biomacromolecules [6]. These structural correlations are not only consistent with the peculiar features of the biomimetic composite but are also compatible with biogenic systems.

In the following we elucidate on the elongated hexagonal-prismatic seed of the fractal growth series and its inner architecture. The seed represents a nanocomposite superstructure ( $\sim 10$  nm – 15 nm) which consists of self-similar subunits (nano-rods,  $\sim 10$  nm – 15 nm in diameter and 300 nm – 350 nm in length) arranged in a close packing to form the seed on the  $\mu\text{m}$ -scale. The nano-rods are nucleated at, and subsequently grow around, the triple-helical fiber protein macromolecules [1,6]. The complexity of the 3D-periodic fluorapatite-gelatine-nanocomposite-superstructure is further increased by an additional pattern consisting of gelatine microfibrils with diameters of around 10 nm [7]. The variations in orientation (and concentration) of the microfibrils lead to a spatial subdivision of the mesoscopic pattern into three distinct areas. Taking into account the experimental evidence for the presence of an electrical potential around the seed [2] the orientation of the microfibrils can be assumed to be controlled by the intrinsic electric field that is generated by the composite during development and growth of the seed. In order to confirm this assumption we focused our work on the following aspects:

- i. TEM investigations of embryonic states of the composite system and their shape development into a hexagonal-prismatic seed [8].
- ii. Simulation of the formation of the hierarchical fibril pattern within the 3D nanocomposite superstructure [7,9].

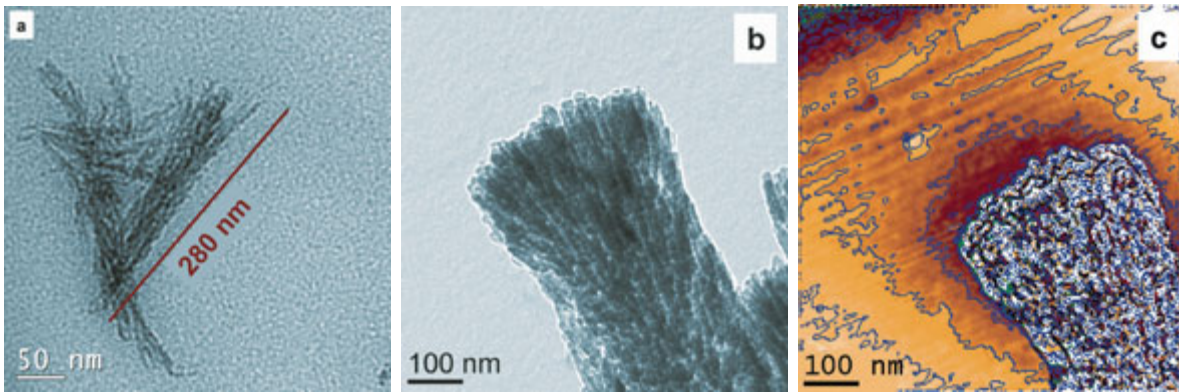


Fig. 1 a: Mineralised bundles of triple-helical macromolecules (typical length  $\sim 280$  nm) embedded in a gelatine-gel matrix visualized by TEM (staining by uranyl acetate); b: TEM image of a (platy) aggregate ( $\sim 350$  nm x 1300 nm) of composite nano-boards in a more or less parallel arrangement; c: Phase image reconstructed from an electron hologram around aggregate (b) showing the tendency to develop a (slightly distorted) electric dipole field.

The present report contains short summaries on these two topics (i. and ii.). Two more brief paragraphs have been added which deal with increased chemical complexity (iii.) as well as with precipitation processes including pre-structuring effects (iv.):

- iii. Carbonated fluorapatite-gelatine-nanocomposites [10].
- iv. Precipitation of calcium phosphate-gelatine-nanocomposites [11].

### Embryonic states and shape development [8]

In this paragraph we focus on the missing link between atomistic simulations [2] on the one hand and pattern formation on a mesoscopic scale on the other hand. As shown in Fig. 1 the initial states of shape development are characterized by triple-

helical fiber protein bundles which are mineralized step by step. Such bundles generate and fix nanoplatelets of fluorapatite in a mosaic arrangement. After their complete mineralization these bundles form elongated composite nano-boards. In a subsequent step, these boards aggregate to bundles of boards in a more or less parallel alignment. Once a critical size is reached an electric field is developed which, in turn, takes over control and directs the further shape development (see Fig. 1). This kind of electric field-directed growth of the elongated polar nano-boards additionally leads to the formation and inclusion of protein microfibrils into the growing composite aggregate. The further shape development (see sketch in Fig. 2) is characterized by adding composite nano-boards, thereby especially increasing the third dimension in volume until a perfect (elongated) hexagonal-prismatic seed is formed.

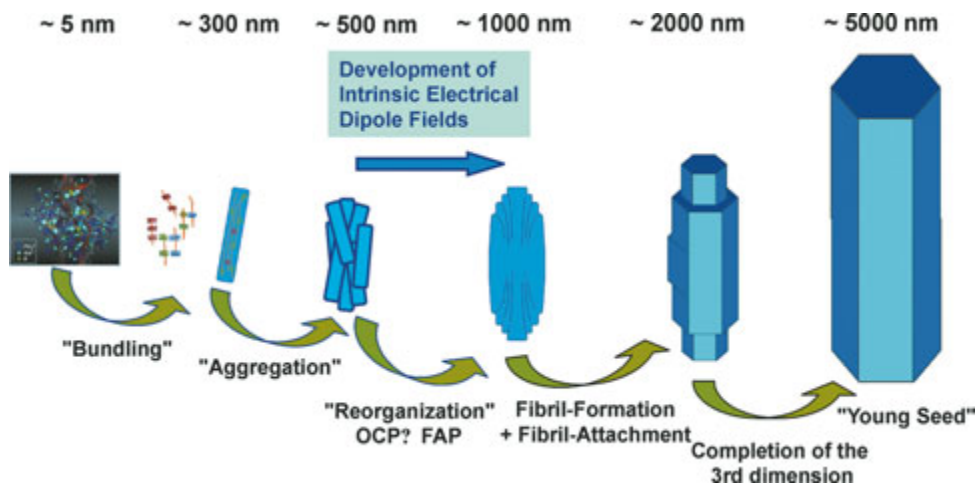


Fig. 2: Scheme of the shape development of fluorapatite-gelatine-nanocomposites. From atomistic simulations [6] (left) to the formation of a hexagonal-prismatic seed (right). Values on top represent the approximate lengths of the various growth-states.

### Hierarchical fibril pattern [7,9,12]

A 2D section of the hierarchical fibril pattern within the 3D nano-composite superstructure of a hexagonal-prismatic seed is shown in Fig. 3. The different orientations of the microfibrils lead to a spatial subdivision of the young seed consisting of three distinct areas (1-3):

1. A central cone-like area containing microfibrils running along the *c*-axis direction.
2. An area with bent microfibrils opening like a flower and extending along the direction of the edges between basal and prism faces.
3. The “waist” area where microfibrils arrange themselves to finally adopt an orientation perpendicular to the prism face.

In order to get deeper insight into the formation and the 3D distribution of the fibril pattern inside a seed we started our simulations on the basis of the experimental findings [1,7]: Elementary building blocks for the aggregation are represented by elongated hexagonal-prismatic objects (A-units), with the embedded triple-helices at their centers. The interactions of the A-units are consequently modelled by three contributions: the crystal energy part (originating from the pair-wise interactions of the apatite shells of the prismatic units), the electrostatic interaction (originating from the unit

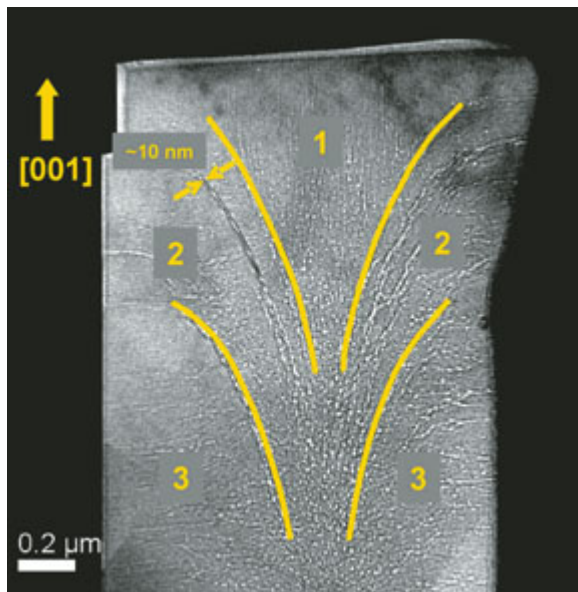


Fig. 3: TEM image of the upper part of a FIB thin cut parallel [001] of a composite seed. Yellow lines indicate the borders between the distinct areas 1-3 representing different orientational characteristics of the microfibrils. For further details see text.

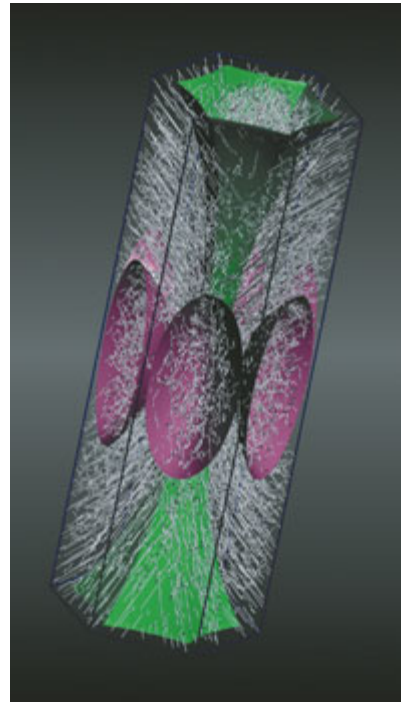


Fig. 4: Simulated 3D fibril pattern within a composite seed. For further details see text.

charges located at the ends of the collagen triple-helices), and the interaction energy of the A-units mediated by the solvent. The next level of complexity is related to the microfibrils consisting of bundles of triple-helical protein molecules, which are embedded within the 3D arrangement of the A-units. The microfibrils are considered as chains of flexible dipoles with effective dipole moments. The growth process is then modelled as energetically controlled stepwise association of elementary building blocks of different kind ( $\alpha$ - and  $\beta$ -dipoles, respectively) on a 3D-grid [9]. The remarkable and excellent qualitative agreement between simulated fibril patterns and our observations by SEM and TEM support the concept of an intrinsic electric field driven morphogenesis of the fluorapatite-gelatine-nanocomposite. The result of a more detailed analysis [12] of the fibril pattern within a composite seed is shown in Fig. 4. The areas 1-3 as defined in Fig. 3 (TEM image) are now clearly identified as an elongated hexagonal saddle-prism (1 in Fig. 3, green in Fig. 4), and as hyperbolic bowls (3 in Fig. 3; pink in Fig. 4), respectively.

The remaining space (containing the bent microfibrils opening like a flower) corresponds to area 2 in Fig. 3. In addition, the simulated fibril pattern may pave the way for fresh attempts to find

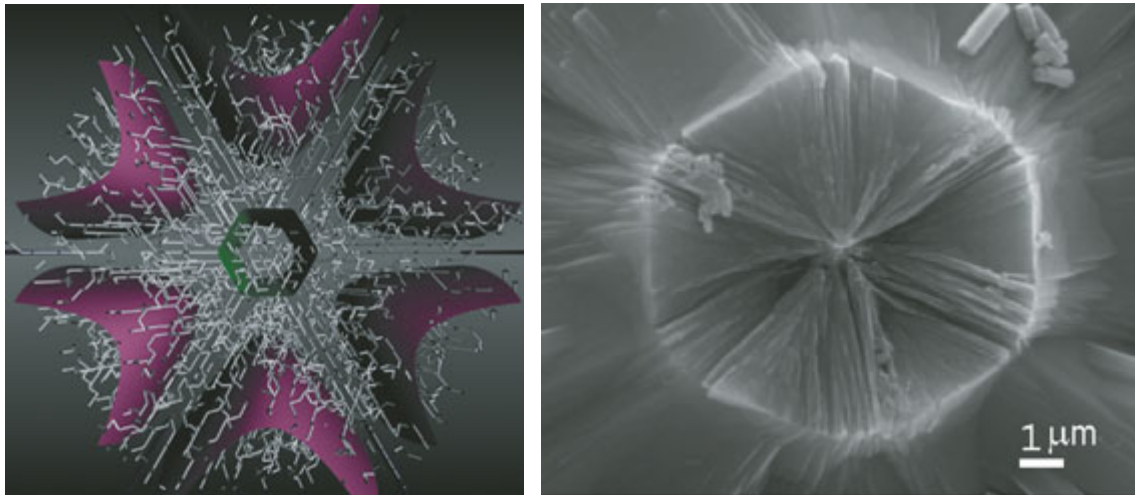


Fig. 5: Cut through the “waist” area (close to the mirror plane perpendicular  $[001]$ ) of the simulated fibril pattern (left) in comparison with a SEM image of the fracture area of the central seed of a fractal composite aggregate (right).

explanations for those experimental observations which are not yet understood, such as the fracture pattern of the central seed of a fractal composite aggregate (see Fig. 5).

For a more quantitative comparison of the simulation results with the experimental data, we started to prepare thin slices of “young” (hexagonal prismatic) composite seeds with well-defined orientations. To accomplish precise cuts, a FIB system was employed. The TEM images of the FIB slices were then overlaid by the simulated patterns of the sections of the volume areas (hex-

agonal saddle prism and hyperbolic bowls) with the same orientation, and by extending the functions derived from the simulation procedure to the  $\mu\text{-scale}$ . The respective results for the thin slices parallel to and around ( $\pm$ ) the  $(001)$  mirror planes of composite seeds clearly show (see Fig. 6) the excellent agreement between simulated patterns and the TEM images. This nice agreement certainly gives a fresh impetus to further develop the *in silico* scenario for the simulation of the fractal shape development (outgrowth and splitting) of the composite seed.

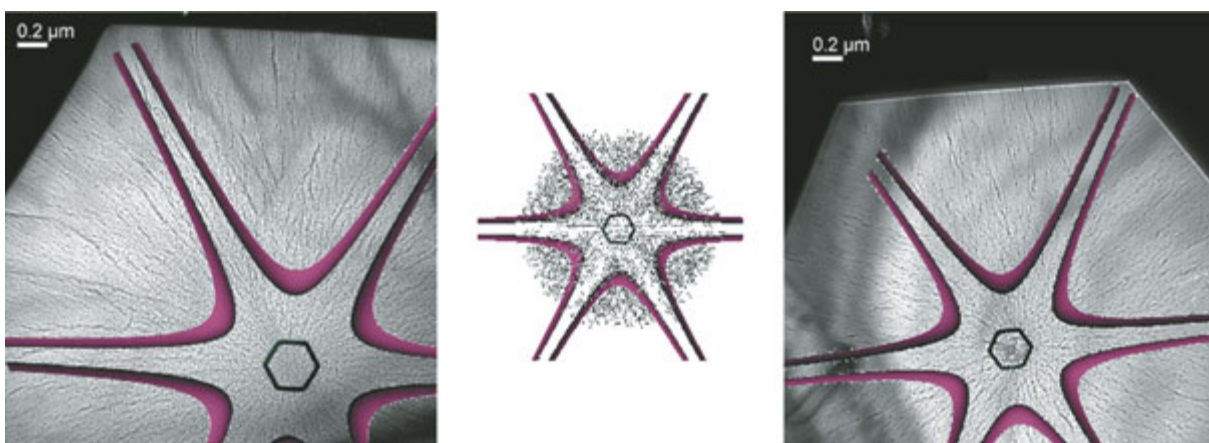
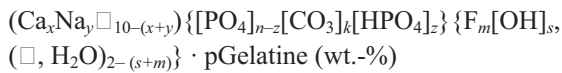


Fig. 6: Thin slices parallel to (and around) the  $(001)$  mirror plane of composite seeds. Center: simulated fibril pattern together with spatial subdivision (sections through the hexagonal saddle prism and the hyperbolic bowls). Left/right: TEM images (thin slices of different composite seeds with the same orientation) overlaid by the simulated spatial subdivisions. For further details see text.

**The effect of carbonate [10]**

In order to investigate materials with chemical compositions that are closer to human hard tissues we also analyzed carbonated fluorapatite-gelatine nanocomposites (morphogenesis as well as structural and chemical properties). This advance increased the complexity of the system significantly which is already clearly reflected by the general empirical formula of the composite:



where  $x = 8.75-9.77$ ;  $y = 0.24-0.49$ ;  $n = 4.80-5.99$ ;  $k = 0.01-1.20$ ;  $z = 0.99-0.22$ ;  $m = 2-1.73$ ;  $s < 0.2$ ;  $p = 2-3$ ;  $(x + y) \leq 10$ ;  $(m + s) \leq 2$ ;  $(n + k) = 6$ ;  $z = (12 + n + s + m - 2x - y)$ .

Carbonate substitution exclusively occurs at the phosphate positions (so-called B-type substitution). The morphogenesis of the carbonated fluorapatite-gelatine nanocomposites follows the fractal as well as the fan-like [5] growth principles. An essential difference with respect to the non-carbonated composites is given by the significantly more flattened and rounded shape of the aggregates. This observation can be explained by the fact that the

carbonated composite aggregates contain nanosubunits that are significantly smaller in length compared with the non-carbonated nanosubunits. In more detail: The coherence length of the nanosubunits along [001] decreases from approximately 300 nm to 70 nm with increasing carbonate content from 0.06 wt.-% to 4 wt.-%. In contrast, the coherence length of the nano-domains along [100] is almost independent of the carbonate content and amounts to approximately 30 nm (see Fig. 7). Thus, we speculate that the change of the morphology of the carbonated composite aggregates may be due to the less anisotropic (less elongated) habit of the nanosubunits, following the general principle of self-similarity.

**Shape- and phase-control by precipitation [11]**

It was already shown [5] that pre-impregnation of gelatine by calcium- and phosphate-ions causes significant morphological changes of the composite aggregates. As the composite material is of interest for medical applications (see Introduction) we investigated the formation of the composite (without fluoride!) by precipitation reactions (preparation of larger amounts of the composite with constant quality).

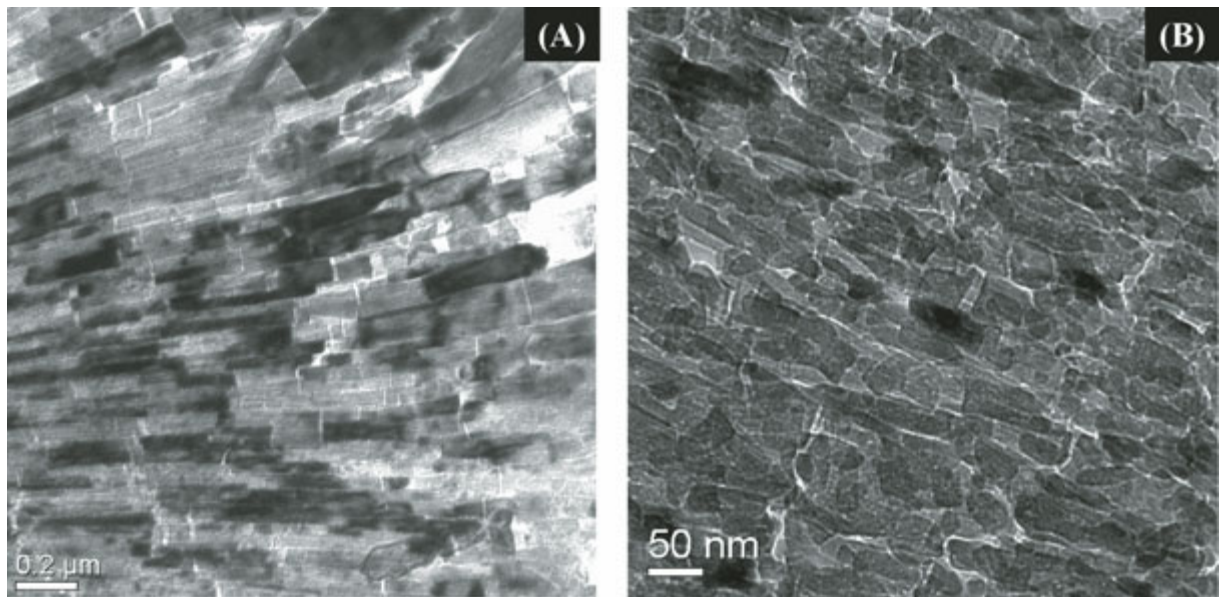


Fig. 7: TEM images (ultra thin slices) of areas of fractal aggregates of fluorapatite-gelatine composites with different carbonate content, indicating differences in nano-structuring of the composites. Carbonate contents: (A) ~ 0 wt.-%; (B) ~ 4 wt.-%. For further details see text.

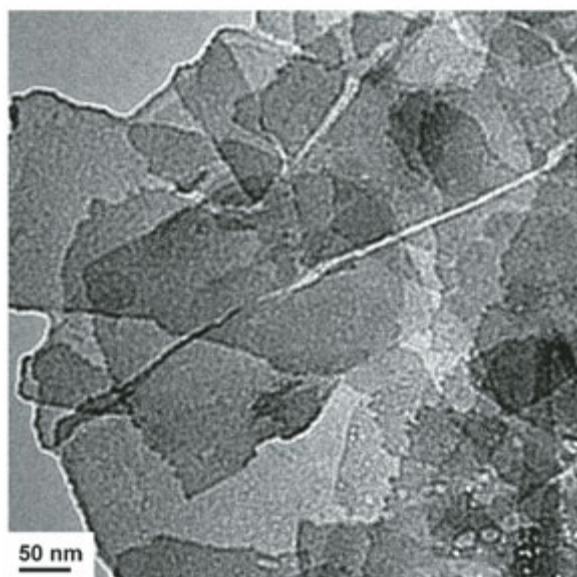
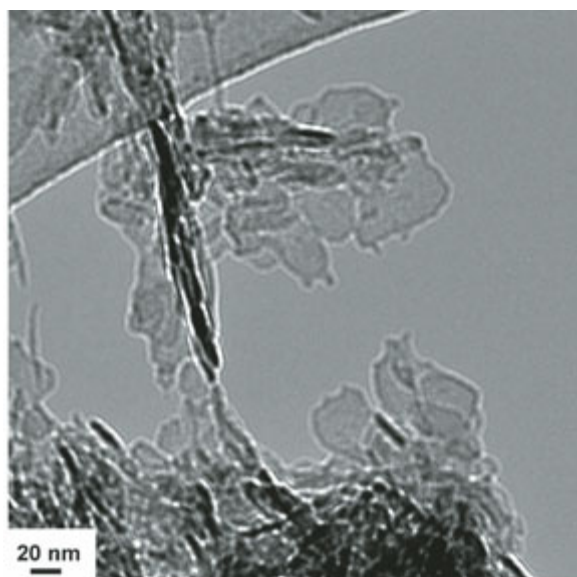


Fig. 8: TEM images of composite particles (without fluoride) prepared by pre-structuring of gelatine with calcium (top; HAP-composite) and by pre-structuring of gelatine with phosphate (bottom; OCP-composite as obtained with higher gelatine quantities in solution). For further details see text.

The composite particles obtained by precipitation reactions are grown with a platy habit. Independent of the amount of gelatine in solution pre-structuring with calcium leads to a hydroxyapatite (HAP) composite (small platelets,  $\sim 50 \text{ nm} \times 30 \text{ nm}$ ). In case of pre-impregnation with phosphate, HAP-composite platelets ( $\sim 60 \text{ nm} \times 30 \text{ nm}$ ) are obtained in the presence of small gelatine quantities, while large quantities of gelatine

prompt the formation of octacalciumphosphate (OCP) composite foils ( $\sim 700 \text{ nm} \times 400 \text{ nm}$ ). Representative TEM images are shown in Fig. 8. The thickness of the platy composite particles ranges from 2 nm to 13 nm (determined by electron holography). In analogy to related biogenic systems containing nano-platelets of calcium phosphates (HAP and OCP), the *c*-axis directions of HAP (hexagonal) and OCP (triclinic) run within the plates (parallel to the platy faces).

## References

- [1] R. Kniep and P. Simon: Fluorapatite-Gelatine-Nanocomposites, in *Biomimetalisation I*, (Ed.: K. Naka), *Top. Curr. Chem.* **2007**, pp.73-125, Springer, Heidelberg.
- [2] P. Simon, D. Zahn, H. Lichte, and R. Kniep, *Angew. Chem.* **118** (2006) 1945-1949; *Angew. Chem. Int. Ed.* **45** (2006) 1911-1915.
- [3] A. Kawska, J. Brickmann, R. Kniep, O. Hochrein, and D. Zahn, *J. Chem. Phys.* **124** (2006) 024513-7.
- [4] D. Zahn, O. Hochrein, A. Kawska, J. Brickmann, and R. Kniep, *J. Mater. Sci.* **42** (2007) 8966-8973.
- [5] As a consequence, a new growth mechanism, the so-called fan-like mechanism, appears. H. Tlatlik, P. Simon, A. Kawska, D. Zahn, and R. Kniep, *Angew. Chem.* **118** (2006) 1939-1944; *Angew. Chem. Int. Ed.* **45** (2006) 1905-1910.
- [6] A. Kawska, O. Hochrein, J. Brickman, R. Kniep, and D. Zahn, *Angew. Chem.* **120** (2008) 5060-5063; *Angew. Chem. Int. Ed.* **47** (2008) 4982-4985.
- [7] R. Kniep and P. Simon, *Angew. Chem.* **120** (2008) 1427-1431; *Angew. Chem. Int. Ed.* **47** (2008) 1405-1409.
- [8] P. Simon, E.V. Rosseeva, J. Buder, W.G. Carrillo-Cabrera, and R. Kniep, in preparation.
- [9] R. Paparcone, R. Kniep, and J. Brickmann, *Phys. Chem. Chem. Phys.* **2009**, DOI:10.1039/B817723F
- [10] E.V. Rosseeva, J. Buder, P. Simon, U. Schwarz, O. V. Frank-Kamenetskaya, and R. Kniep, *Chem. Mater.* **20** (2008) 6003-6013.
- [11] T. Kollmann, P. Simon, W.G. Carrillo-Cabrera, C. Braunbarth, T. Poth, and R. Kniep, in preparation.
- [12] R. Paparcone, S. Kokolakis, P. Simon, W.G. Carrillo-Cabrera, R. Kniep, and J. Brickmann, in preparation.

<sup>1</sup> Technische Hochschule Darmstadt

<sup>2</sup> University of St. Petersburg, Russian Federation

<sup>3</sup> Technische Universität Dresden

<sup>4</sup> Sustech GmbH, Darmstadt